Research Square

Preprints are preliminary reports that have not undergone peer review.
They should not be considered conclusive, used to inform clinical practice,
or referenced by the media as validated information.

Uncertainty in the Regional Consequences of Atlantic Overturning Decline

Jonathan Rosser

j.p.rosser@lse.ac.uk

London School of Economics and Political Science https://orcid.org/0000-0002-7748-319X

David Stainforth

London School of Economics https://orcid.org/0000-0001-6476-733X

Article

Keywords:

Posted Date: November 19th, 2026

DOI: https://doi.org/10.21203/rs.3.rs-11378213/v1

License: This work is licensed under a Creative Commons Attribution 4.0 International License.
Read Full License

Additional Declarations: There is **NO** Competing Interest.

Uncertainty in the Regional Consequences of Atlantic Overturning Decline

Jonathan Rosser[1*] and David Stainforth[1]

[1]Grantham Research Institute, London School of Economics, Houghton Street, London, WC2A 2AE, United Kingdom.

*Corresponding author(s). E-mail(s): j.p.rosser@lse.ac.uk;
Contributing authors: D.A.Stainforth@lse.ac.uk;

Abstract

The potential "collapse" of the Atlantic Meridional Overturning Circulation (AMOC) has significant implications for climate change policy but diverse perspectives exist in the scientific community regarding its likelihood, timing, and impacts. To reflect these differing interpretations of the evidence base, policy-relevant assessments need to be applicable to a wide-range of scenarios of future AMOC behaviour - including hypothetical behaviour not reflected by today's earth system models.

Here we provide a framework for assessing the regional consequences of such scenarios of AMOC change within the context of diverse scenarios of greenhouse gas driven warming. We show that for a large AMOC decline (12 Sv in the 21st century) within the SSP245 warming scenario, today's model simulations imply a very wide range of outcomes for Northern Europe: from 2°C warming to 12°C cooling relative to the present day. In other regions, the responses are more muted; in South Asia we find warming of between 1°C and 4°C.

We cannot put decision-relevant probabilities on these results but we demonstrate how different assumptions relating to the epistemic interpretation of model ensembles substantially affect the conditional, model-based, probabilities of different outcomes. Our methodology represents a new tool for generating policy-relevant, uncertainty-focused assessments of the consequences of potential future AMOC changes, thereby enabling the differing perspectives in the research community to be translated into the impacts at the heart of wider societal discourse on the subject.

1 Introduction

The potential consequences of large changes in the Atlantic Meridional Overturning Circulation (AMOC) are an important source of uncertainty in climate change impact assessments. Indeed, estimates of the societal impacts of AMOC reductions alone vary widely from severe economic losses to net global benefits [1–4]. Such assessments are founded on simulations of physical impacts in a small set of Earth System Models (ESMs) but the sensitivity of AMOC to greenhouse-gas-induced warming is widely debated in the scientific community and these models do not reflect the range and timing of future AMOC reductions considered plausible[2, 5–11]. A key challenge in climate change science - and one which has significant policy relevance - is therefore to provide assessments of regional impacts that reflect the diversity of behaviour in the ESMs while also being applicable to a diverse set of future AMOC scenarios beyond those simulated within them.

Here we provide a framework for assessing the regional changes resulting from a user-defined combination of greenhouse-gas-induced warming (such as that resulting from one of the shared socio-economic pathways (SSPs) [12]) and AMOC change (such as the hypothetical large reduction considered in this study). Our approach integrates a variety of model-based lines of evidence but crucially the assumptions on how model data is used are transparent and can be easily adjusted to reflect the opinions of individuals or groups of experts. The framework therefore also represents a tool for the future generation of a collection of expert-based, subjective Bayesian assessments of the impacts of AMOC change within a warming world.

Previous studies of the regional consequences of AMOC change have looked at either single model experiments [3, 13], or small multi-model ensembles but only in pre-industrial climates i.e. with no greenhouse gas (GHG) driven climate change [14]. Neglecting the interaction with GHG driven warming is likely to be critical since global warming influences AMOC strength and may influence its regional impacts. We are interested in the combination: the regional consequences of AMOC reduction in a warming world. Furthermore, these experiments have no, or only very limited, assessments of the consequences of epistemic, model-formulation uncertainty. Current models incompletely sample structural and dynamical uncertainty; for instance, they omit key processes such as ice sheet interactions [15, 16], and likely exhibit common biases, which may include a bias towards stable AMOC behaviour [17, 18]. We therefore a priori expect our existing estimates of impacts to fail to capture the range of possible outcomes that we should consider plausible given today's knowledge.

The framework introduced here allows quick exploration of AMOC regional impact uncertainty in any chosen future scenario. By integrating information extracted from GHG driven modelling experiments with information from modelling experiments targeted at AMOC change (under both pre-industrial and warming scenarios), the framework captures the relationships between GHG-driven global warming, AMOC, and regional temperatures. This enables a much fuller exploration of uncertainty than looking at ESM output directly, although it is still, of course, limited by the model simulations available.

We begin by introducing the framework and how existing model experiments can be used to inform the relationships within the framework (Section 2), and then use

these relationships to explore the uncertainties in the regional consequences of an arbitrary but substantial degree of AMOC reduction in the context of a middle-of-the road scenario for GHG-driven warming (Section 3). We finish with a discussion of the potential of this approach to capture epistemic uncertainty in the consequences of an AMOC "tipping point", and of the implications more broadly for the interpretation of earth system model based climate projections (Section 4).

2 AMOC Impacts Framework

The pattern of regional temperature changes associated with changes in AMOC is expected to be different to that resulting from greenhouse gas (GHG) driven global warming alone [13]. The two are not, however, independent. One can imagine a hypothetical pattern of regional temperature changes resulting from GHG-driven warming in the absence of AMOC changes (orange region in Figure 1), but in practice GHG-driven warming is expected to induce changes in AMOC so the realised regional consequences will be a combination of both drivers (orange and green regions in Figure 1). Indeed the connection between global mean surface temperature (GMT) change and AMOC is expected to be bi-directional: in climate models increasing global temperature typically weakens the AMOC, while decreasing AMOC typically decreases the global temperature (green arrows in Figure 1). The existence of ESM simulations driven by changing GHGs alone and another set of simulations driven by changes in AMOC alone allows us to isolate the different patterns of regional temperature change and the bi-directional feedbacks between AMOC and GMT. The various connections in the proposed framework are illustrated in Figure 1.

The starting point for quantifying these relationships is the collection of model simulations in which changes in AMOC are driven by the idealised input of freshwater into the North Atlantic, so-called freshwater hosing experiments [14, 19–21]. In these experiments, the levels of atmospheric GHGs are held constant, so the situations they represent are the blue and green regions of Figure 1. These experiments provide, directly, estimates of the regional temperature change resulting from a particular change in AMOC (relationship $\delta*$ in Figure 1). If we assume that a change in AMOC induces a change in GMT, and vice versa (as in Figure 1), and that both these relationships are linear, then these experiments also provide a measure of the relationship $\beta*$ in Figure 1 (see Methods for this calculation based on iterative feedback between GMT and AMOC).

By contrast, a different set of model simulations driven by changing atmospheric GHGs (the CMIP6 simulations [22]) represent the situation of the orange and green regions of Figure 1. These experiments provide a measure of relationship $\alpha*$ in Figure 1 (see Methods). They also tell us $\Delta\text{GMT}_{\text{Realised}}$ and $\Delta\text{RMT}_{\text{Realised}}$ - the global/regional change in temperature resulting from a combination of warming-induced AMOC change (herein termed "indirect" effects), and all other GHG-driven changes (herein termed "direct" effects). By combining measures of $\alpha*$, $\beta*$, $\delta*$, and $\Delta\text{RMT}_{\text{Realised}}$ / $\Delta\text{GMT}_{\text{Realised}}$ for the same model we can deduce the direct effects $\Delta\text{RMT}_{\text{GHG}}$ / $\Delta\text{GMT}_{\text{GHG}}$ and thereby a measure of relationship $\gamma*$ for that model.

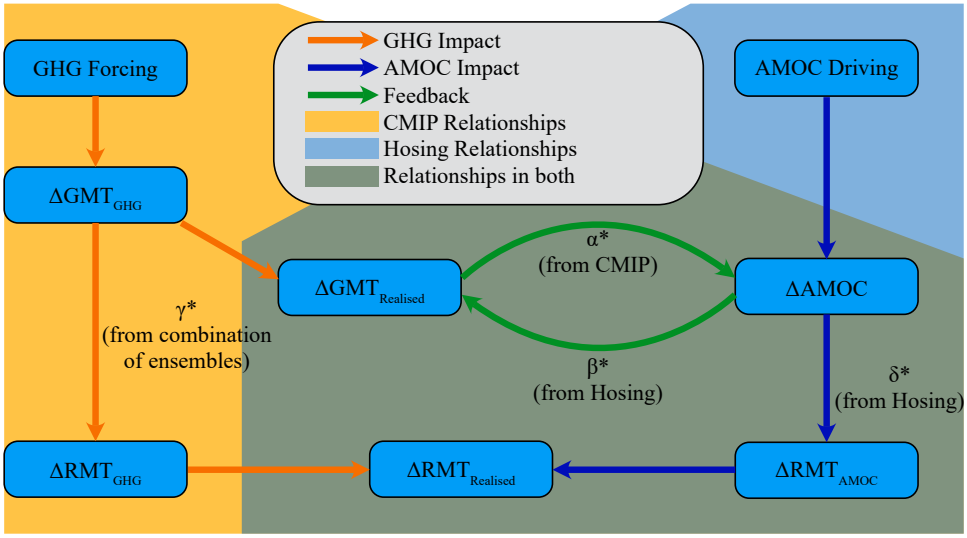


Fig. 1 Framework used to analyse the relationship between AMOC and GMT and to project the response of the regional temperatures. Orange backgrounds illustrate the relationships present in CMIP6 scenarios (SSP245 in this analysis), blue backgrounds those in the hosing experiments, and green backgrounds show relationships present in both. Orange arrows represent the direct impacts of greenhouse gas forcing, blue arrows the direct impacts of AMOC driving, and green arrows the feedbacks between AMOC and realised GMT. Key relationships derived from model data are labelled $\alpha^*, \beta^*, \gamma^*, \delta^*$.

In our analysis, we assume that all the relationships ($\alpha*$,$\beta*$,$\gamma*$,$\delta*$) are linear and also independent of the level of warming or AMOC change (these assumptions are investigated and justified in the Methods). The relationships are assumed to be independent of each other, apart from $\beta*$ and $\delta*$, which both represent the impact of AMOC changes on surface temperature and are thus highly correlated and treated together (explored further in the Methods). We further assume that the feedbacks between AMOC and GMT (relationships $\alpha*$ and $\beta*$) are sufficiently weak to allow a stable or multi-stable state. This is consistent with both the analysis here and previous studies on the stability of the AMOC [23].

The linearity assumptions mean that the relationships ($\alpha*$,$\beta*$,$\gamma*$,$\delta*$) can be represented simply by parameters (α,β,γ,δ), which we calculate by linearly regressing the relevant variables on each other (see Methods) using annual mean data through the length of each simulation. These assumptions are certainly open to question (see, for instance, [24] regarding state-dependent effects) but the model data is broadly consistent with them. Attempting to extract more complex relationships is not justified given the lack of significant deviations from these linearity assumptions in the data and the small sample size (see supplementary figures 4-9 and the more detailed discussion in the Methods), but new model data, or physical understanding, could lead to a different conclusion in the future.

Figure 2, panels C, D, G and H show these relationships for one model (CanESM5). For this model, only one freshwater hosing simulation exists (panels C,D) and hence only a single evaluation of β and δ, but for the GHG-driven experiment (panels G,H)

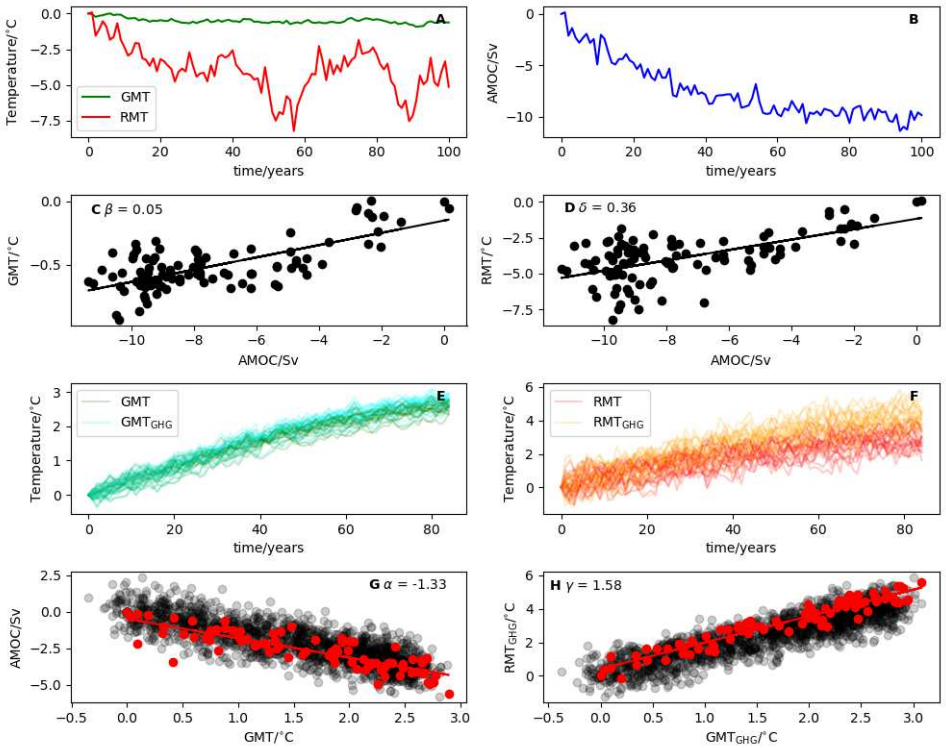


Fig. 2 Steps in the framework for calculating the parameter values α,β,γ,δ(as shown in Figure 1) for a single model (CanESM5). Panel A shows the GMT and Northern European RMT for a hosing run under preindustrial conditions, both showing a decrease, but the decrease is much larger in RMT. Panel B shows the AMOC circulation strength for the same run. Panels C and D show the regressions against AMOC using this data to calculate β (GMT) and δ (RMT). Panels E-H show similar results but for the SSP245 runs of the CanESM5 model. They additionally show the GMT and RMT adjusted for AMOC impacts in Panels E and F, both slightly higher once AMOC impacts are accounted for. In Panels G and H we see the regressions to calculate α (AMOC vs GMT) and γ ($\mathrm{RMT_{GHG}}$ vs $\mathrm{GMT_{GHG}}$). The data for all model initialisations is shown, but as this is calculated on each initialisation separately, one initialisation is highlighted in red to demonstrate how this is calculated for the specific initialisation.

there is an ensemble of simulations (in this case 20 members), so we can calculate multiple evaluations of α and γ (Table 1 - row CanESM5). Equivalent figures for a further six models are presented in the SI (Supplementary Figures 4-9) and the resulting parameter values are given in Table 1. There are unfortunately no ensembles of pre-industrial hosing simulations for any individual model, so we have only one estimate for β and δ for all models other than MPI-ESM1-2-HR, which has estimates at pre-industrial and 2°C of warming. However, four of these models have ensembles of the GHG-driven SSP245 simulations and for these we are able to calculate parameters α and γ for each simulation, thus providing some degree of intra-model uncertainty quantification (Table 1).

Model	α	β	γ (NEU)	δ (NEU)	γ (SAS)	δ (SAS)
Multi-model Ensemble Mean	-1.85 [-2.91,-0.57]	0.06 [0.02,0.14]	1.41 [0.83,2.44]	0.45 [0.01,1.19]	1.12 [1.00,1.28]	0.03 [-0.03,0.09]
CanESM5	-1.43 [-1.76,-1.09]	0.05	1.47 [1.21,1.66]	0.36	1.09 [1.02,1.20]	0.04
CESM2	-0.57	0.14	0.83	1.19	1.20	0.09
EC-Earth3	-2.91	0.03	0.99	0.01	1.09	0.00
HadGEM3-GC31-LL	-2.14 [-2.53,-1.95]	0.05	1.42 [1.31,1.49]	0.22	1.04 [1.00,1.06]	0.04
IPSL-CM6A-LR	-1.42 [-1.48,-1.34]	0.11	2.28 [2.12,2.44]	0.98	1.04 [1.01,1.08]	0.07
MPI-ESM1-2-HR	-2.83	0.04 [0.02,0.05]	1.65 [1.51,1.80]	0.22 [0.18,0.25]	1.16 [1.16,1.17]	-0.01 [-0.03,0.00]
MPI-ESM1-2-LR	-1.65 [-1.96,-1.48]	0.03	1.23 [0.97,1.43]	0.15	1.21 [1.15,1.28]	-0.01

Table 1 CMIP6 models with model runs for SSP245 and hosing scenarios, and the parameters calculated for each of these models. Parameters calculated for α (impact of GMT on AMOC), β (impact of AMOC on GMT), γ (impact of GMT on RMT compensating for AMOC), and δ (impact of AMOC on RMT), with γ and δ calculated for Northern Europe and South Asia. Where multiple values for the parameter could be calculated for a given model, the mean is given, followed by the range. The range is given where multiple SSP245 or hosing runs are available.

Most of the parameters vary substantially across the multi-model ensemble. The interactions between AMOC and GMT (α and β) vary by a factor of more than 5.

For parameters which depend on region (γ & δ), the variability across models is itself very region dependent; for Northern Europe γ varies by a factor of 3 and δ spans orders of magnitude, while for South Asia the parameters are more tightly constrained, or of small but uncertain sign (Table 1). The intra-model ensembles, such as that of CanESM5, show smaller but still substantial variations in the parameter estimations from different individual simulations.

Despite substantial uncertainty, the parameters have physically consistent signs and demonstrate some clear messages:

1. GHG-driven warming leads to AMOC weakening and the direct effect is regional warming which is stronger in regions closer to the poles (Supplementary Figures 1 & 3).
2. AMOC decline leads to cooling in Northern Europe, with smaller impacts in South Asia, often of uncertain sign (Supplementary Figure 2).
3. Decreasing AMOC leads to decreasing GMT in all models (Supplementary Figure 1); this response may be due to associated changes in Arctic sea ice or cloud feedbacks [25, 26].

3 Projections of AMOC Impacts

Having used current model simulations to deduce the relationships α^*,β^*,γ^*,δ^*, we now use them to project a hypothetical future rarely explored in models (fewer than

5% of CMIP6 runs investigated). We choose a scenario of substantial and rapid AMOC decline (12 Sv decrease from 2015 values by the end of the 21st Century) within a middle-of-the-road scenario of GHG emissions (SSP245 [12]). This combination is chosen to illustrate the use of the framework to explore a future with rapid AMOC decline to the lower end considered plausible, displayed only by a small number of model runs[27–29]. We also demonstrate how differing assumptions regarding the interpretation of multi-model ensembles can lead to very different conclusions about the likelihood of different impacts within the scenarios studied. We focus on the IPCC AR6 region of Northern Europe[30] but present other regions in the supplementary information.

To provide a context for our projections we first analyse the CMIP6 simulations under the SSP245 scenario but with only their internally-modelled AMOC decline. The probabilistic interpretation of the CMIP6 ensemble raises widely-discussed epistemic questions [31–34] but for the purposes of illustration only we build a distribution of regional impacts based on each model having equal weight, and that weight being equally distributed across the available simulations of that model's initial condition ensemble (see Methods). Applying this approach to the seven models used in our framework above gives us a point-of-context distribution for the regional mean temperature change in 2090-2100 by comparison to 2015-2025 (Fig 3, CMIP6) .

To evaluate the implications of greater AMOC decline than that generated internally in the ESMs, a common method is to add a single value estimate of the regional impact of AMOC change to a global warming scenario [1, 35]. We call this the "offset method" and use it to generate a further point-of-comparison distribution. Typically the single value will come from a hosing experiment and may be either from a single model simulation or a mean across an ensemble of model simulations. Here we use the CMIP6 SSP245 simulations as our global warming scenario projections (weighted as above) and for the single-value AMOC offset we use the multi-model ensemble mean of the regional temperature change in the hosing simulations of our seven models; again each model is given equal weight (see Methods). The AMOC reductions in these hosing simulations are substantial although typically not as great as the 12Sv decrease of our hypothetical scenario. The resulting distribution (Fig 3, Offset Method) is of course the same as the CMIP6 distribution but simply shifted by the offset. This approach implies that a substantial AMOC weakening could lead to an overall cooling effect in Northern Europe relative to 2015-2025 conditions: -5 to 0°C in 2100 rather than the warming of 0 to 5°C seen in the unadjusted CMIP6 distribution. However, this approach double-counts some AMOC impacts because the CMIP6 SSP simulations already embed a level of AMOC slowdown. Furthermore, it doesn't reflect the diversity of model responses to changes in AMOC; we should therefore expect it to underestimate our uncertainty.

The framework of section 2 provides a more general and flexible way to assess the regional impacts of AMOC decline - one which doesn't double count and better captures the diversity of model responses. Taking the models one at a time, the framework provides values for the parameter set (α,β,γ,δ) for each combination of CMIP6 simulation and hosing simulation. Each set of parameters, combined with its associated CMIP6 SSP245 $\Delta\mathrm{GMT}_{\mathrm{Realised}}$ value for the end of the century and the hypothetical

AMOC decline (-12Sv by 2100), leads to a projection of regional temperature change (Methods). Weighting these projections in the same way as the CMIP6 simulations above (i.e. equal weight to each model) generates a distribution of impacts for our hypothetical scenario (Fig 3, Individual Projections). Several points are worth noting about the distribution for Northern Europe. First, while the CMIP6 distribution is essentially continuous, this "individual projections" (IP) distribution is substantially discontinuous: there are large gaps which reflect the very different responses to AMOC change in the different models. Second, some models lead to vastly greater impacts so the distribution spans a wide range of -12 to +2 °C (much wider than the -5 to 0 °C of the offset method) and includes the possibility of simply reducing the impact of global warming rather than overall cooling. Third, the offset distribution aligns with a gap in the IP distribution implying that the offset method can generate responses that are inconsistent with all of its underlying models.

The gaps in the IP distribution highlight the already well recognised need for a greater diversity of ESMs and/or associated perturbed physics ensembles to inform our uncertainty in the response of the climate system to increasing atmospheric greenhouse gases [36–38]. They also highlight the need to reflect on the epistemic choices we make when interpreting multi-model ensembles; something which our framework is well suited to illustrate. Rather than taking the individual-model-outcomes-with-equal-weighting approach above, we could instead sample the parameters α,β,γ,δ according to some probability distribution and in combination with the whole collection of CMIP6 SSP245 $\Delta GMT_{Realised}$ values. This we do here using three different probability distributions for the parameters. First is a uniform distribution which arises from an interpretation of the model-derived parameter values as providing only a range of possibilities (see Katzav et al and Stainforth, 2007 for a discussion of possibilistic interpretations [31, 34]) across which we choose to assign a uniform probability. Second and third are gamma and normal fits to the collection of model-derived parameter values, which, while still giving the models equal weight, assumes both that they are samples from a distribution and the shape of that distribution. These assumptions are open to question, as is the equal-weight assumption, but they are valuable for illustrating the consequences of our epistemic choices. These choices may be founded on lines-of-evidence beyond the models. The gamma distribution, for instance, is included because it allows the sign of the parameter to be constrained, something which in some cases may be justified by physical reasoning.

The resulting distributions (Figure 3, Uniform, Gamma, Normal) avoid, by design, the gaps in the IP distribution, but the bulk of the probability mass lies in the same -12 to +2°C range. However, the shapes of the distributions differ substantially. The uniform parameter distributions lead, unsurprisingly, to a flat response distribution; the gamma and normal both lead to peaked distributions although their peaks are in different places. The extremes of the response distributions show particularly pronounced differences, with the uniform having tightly constrained tails, the gamma showing a long tail to extreme cooling scenarios, and the normal showing wide but symmetric tails to strong cooling and warming. Notably, even the uniform response distribution has tails that go well beyond the response range of the individual projections - particularly on the warming side.

A further, key epistemic choice in interpreting ESMs is simply which ones to include in the analysis. Our seven models were chosen because they were the only ones available with both SSP245 and hosing simulations. However, one might argue that some of these models are insufficiently representative of reality to be included in the analysis. We illustrate the substantial consequences of such a decision by excluding the two models that show the most substantial regional cooling in Northern Europe in response to hosing (Figure 3, grey distributions); this can be viewed as an extreme application of model-weighting. Excluding these models from the analysis makes little difference to the CMIP6 distribution but the offset distribution is now shifted to span no change (-1°C to 2°C); this is because the offset is taken as the ensemble mean impact in the hosing experiments and the ensemble is now much smaller because it no longer includes the two extreme models. Similarly, the IP distribution is now tightly constrained around no change (-1°C to 2°C). The response distributions based on sampling parameter distributions are also much more constrained, span no change, and are now almost independent of the parameter distribution chosen. The majority of the density is thus around -3°C to 3°C in all methods, although it is less well explored in the offset method. These results clearly illustrate how the conclusions drawn from a multi-model ensemble can depend dramatically on the choices made regarding how the sample is interpreted; in particular they can be strongly impacted by the behaviour of one or two particular models. However, since all our models are substantially different to reality there is no clear way of omitting only a few so we are left with large ranges of possible behaviour and deep uncertainty in the representative response probability distribution.

4 Discussion

No climate model can accurately project the probability distributions representative of future climate conditioned on real-world physics and a scenario of future GHG emissions, so it is critical to generate projections of the fullest possible range of future climates by maximally exploring model diversity. When trying to explore this range with our current models some behaviours and responses are not simulated. These may be in regions beyond the bounds of the current model responses or they may be unsimulated behaviour within the range of current model responses - as illustrated by the gaps in the "Individual Projections" approach above. These gaps may be"physical" in the sense that they represent behaviour and responses that are not consistent with the physical world. They may, alternatively, be due simply to a lack of model diversity, limited ensemble size, or limited physical understanding. Increased model diversity can help to improve our understanding of these gaps and determine which are physical and relevant for decision and policy support, and which are a result of our limited exploration of possibilities. Single model studies cannot explore the range of possible response behaviour, and therefore represent a very limited assessment.

Of course, current understanding about future climate does not derive solely from complicated climate models. The potential for rapid AMOC decline, for instance, is something that can be analysed from a variety of different perspectives. This paper

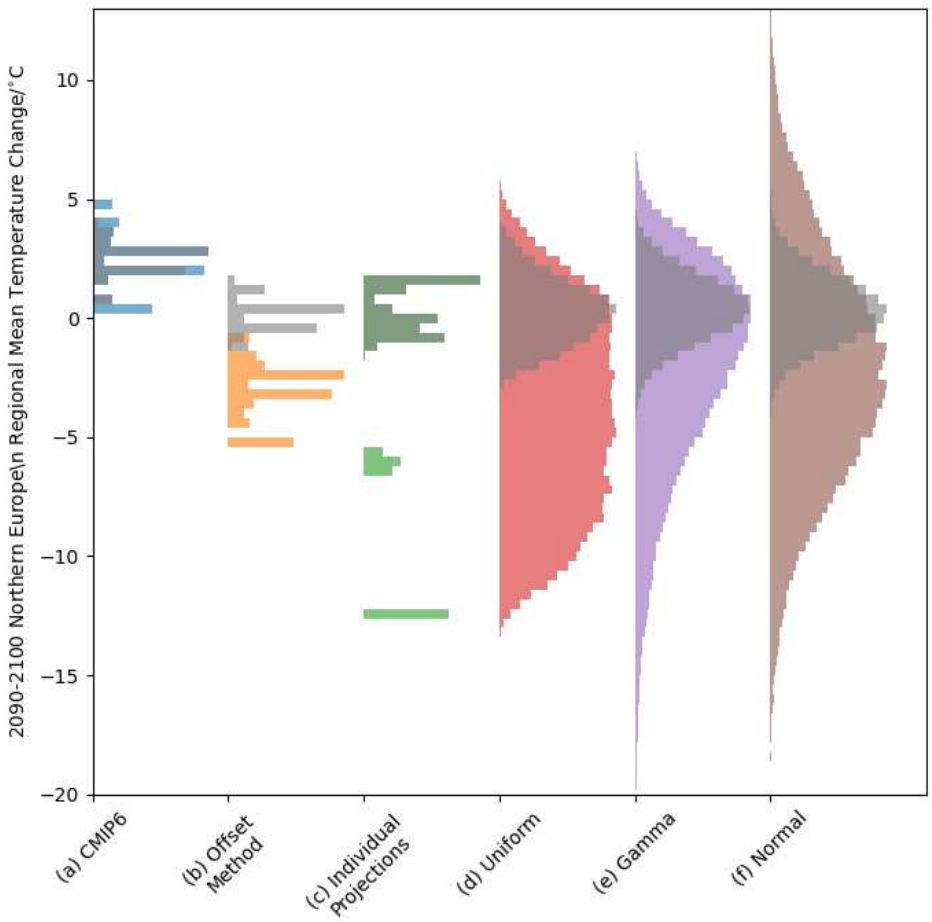


Fig. 3 Histograms of the 2090-2100 regional mean temperature change relative to 2015-2025 in (a) the unadjusted CMIP6 SSP245 runs and (b-f) an SSP245 scenario combined with large AMOC decline (-12Sv). In the latter (b) uses the offset method and (c-f) our disaggregation framework. The different applications of the framework are: (c) "individual projections" made by applying the framework to each model individually and then combining the results into one distribution, (d) utilising a uniform distribution for each of the framework parameters, (e) utilising a gamma distribution fit to each parameter, and (f) utilising a normal distribution fit to each parameter. The coloured histograms show the density of outputs when all models are included. The underlying grey histograms show the results for the same approaches but with the two most extreme models removed (CESM2 and IPSL-CM6A-LR).

illustrates a conceptual framework that facilitates clearer integration of diverse information sources; sources which can include dynamical understanding, a hierarchy of modelling approaches, observational analyses and paleoclimate constraints. Such integrated information could drive the scenarios explored in our framework and thereby provide more robust information for societal debates around climate change: information that more fully reflects the breadth of relevant scientific understanding. At

the same time, further exploration of integrated global warming and AMOC change scenarios through earth system modelling experiments would allow the structure and uncertainty exploration of the framework to be improved. Furthermore, similar frameworks could be created for other impacts, such as the precipitation response to AMOC changes, and for other drivers, such as a die-back of the Amazon Rainforest.

Our framework illustrates the fundamental importance of the underlying assumptions made in multi-model assessments. The results we have presented vary substantially according to the method used to integrate model-based information, the assumptions made about the existence or not of a relevant underlying distribution that reflects reality, and which models are included. More generally, questions of model inclusion, weighting and independence are likely to have first-order impacts on the outcomes and messages of such studies. We can pick out three key messages in this respect. First is the need for transparency about the underlying assumptions; this is essential to facilitate informed debate and informed interpretation of the results. Second is the importance of sensitivity studies regarding those assumptions if their impact is to be interpretable.

Third is the importance of pushing out the bounds of model response behaviour so that questions of credibility and relevance can be studied, and a degree of robustness associated with the conclusions. Of course, all current models have flaws that would allow them to be reasonably ruled out as inconsistent with reality (large biases, key missing components such as ice sheets, and unresolved processes) so the question of pushing out the bounds becomes one of judging when a model is sufficiently realistic/unrealistic to be included/excluded.

In some cases, choices around model interpretation and epistemic assumptions may have little impact on the outcomes. For example, when the most extreme models are removed from the analysis herein, the choice of parametric distribution or interpretational approach doesn't change the temperature impact significantly from the -3 to 3°C range. This suggests that, under these assumptions, the result is relatively robust. However, even with this agreement, the result must be interpreted with care as the lack of variation could be due to model clustering or, as is evidenced here, an incomplete sampling of possible models. For AMOC analysis, this study demonstrates that in many regions there are a wide range of model outcomes and the epistemic assumptions are crucial for the conclusions drawn.

The framework presented herein enables the exploration of regional consequences of hypothetical scenarios of AMOC change. To improve this framework, it should be established which hypothetical scenarios and dynamical relationships are credible and which are too unrealistic to be relevant for policy. This requires bringing together experts across relevant disciplines to discuss and refine potential ranges of dynamical behaviour and plausible scenarios. Increasing model diversity would also enable better exploration of the dynamical behaviour and domain of possible climate outcomes. However, even with the existing data and understanding, decisions and policies must be made and the tools of Decision Making under Deep Uncertainty (DMDU) exist to address this situation. Linking such methods to scientific efforts to better understand and quantify uncertainty would have significant value in responding to the threats of climate change. The framework presented here, and potentially related frameworks for

other elements of the system, could aid these approaches. An important scientific challenge, therefore, is to further align research with decision-making, whether by exploring the domain of possible responses, investigating the range of scientific uncertainty, or focusing scientific research methods on climate features critical to decisions.

5 Methods

5.1 Data

North Atlantic freshwater hosing scenarios under pre-industrial conditions were taken from the NAHosMIP scenarios [14], which yielded model runs from eight different models. North Atlantic freshwater hosing scenarios were also taken from the ClimTip ensemble, which follows the Tipping Points Model Intercomparison Project (TipMIP) protocol for the response to hosing under a 2°C level of global warming [19–21]. It follows the novel temperature stabilisation protocol before applying identical hosing to that in the NAHosMIP runs. There were 3 models available for this, each with a single run. Models from the NAHosMIP or ClimTip ensembles with available ssp245 runs were used for the entire analysis (7 models in total, 7 from NAHosMIP and 1 additional model run from ClimTip) while two models (CESM1-CAMS and HadGEM3-GC31-MM) were used only for comparison of the response to hosing under different levels of global warming.

The CMIP6 (Coupled Model Intercomparison Project 6) SSP245 (Shared Socio-Economic Pathway) scenario was used [12] to explore the response to radiative forcing. For each of the models for which hosing experiments were available, SSP245 model runs were selected based on their availability on the CEDA archive on JASMIN [39], with some supplementation for key models to allow better comparison across the hosing and greenhouse gas forcing experiments (models utilised summarised in Supplementary Table 1).

The IPCC AR6 climate reference regions [30] were used for bounding the area-weighted regional mean temperatures.

5.2 Calculation of Input Variables

The Atlantic Meridional Overturning Circulation was calculated on depth levels and was calculated as the maximum of the Atlantic z-level streamfunction at the latitude closest to 26.5°N on the model grid, excluding the top 200m (this was done using the msftyz standard variable outputted from CMIP-class models).

The area-weighted regional mean temperature was calculated by the area-weighted average of the surface air temperature of cells which overlap with the given region (using the tas and areacella standard CMIP variables).

The global mean temperature was calculated as an area-weighted mean of the surface temperature over the entire globe/ model grid.

5.3 Relationship Calculations and Assumptions

5.3.1 Impact of GMT on AMOC

To calculate the impact of GMT on the AMOC, we use the CMIP6 SSP245 scenario to force the GMT with changing greenhouse gases and observe the outcome. We treat this as an intervention in the radiative forcing, directly influencing the surface temperature and thus indirectly influencing the AMOC. By assuming that the change in the AMOC is mediated by the change in radiative forcing and hence global temperature, a relationship can be calculated between GMT and AMOC, as shown in Figure 1. By assuming linearity the impact of the feedbacks between AMOC and the realised GMT can be calculated using the following relationship:

$$\begin{aligned}\Delta\text{GMT}_{\text{Realised}} &= \Delta\text{GMT}_{\text{GHG}} + \alpha\beta * \Delta\text{GMT}_{\text{GHG}} + (\alpha\beta)^2\Delta\text{GMT}_{\text{GHG}} + ... \\ &= \Delta\text{GMT}_{\text{GHG}} * (1 + \alpha\beta + (\alpha\beta)^2 + ...) \\ &= \Delta\text{GMT}_{\text{GHG}}/(1 - \alpha\beta)\end{aligned}$$

This relationship assumes that a change in the greenhouse gas forced GMT is adjusted through the feedback loop, leading to an equilibrium or quasi-equilibrium state with an adjusted GMT ($\Delta\text{GMT}_{\text{realised}}$) which is different to the counterfactual GMT seen if the AMOC hadn't changed (which we have labelled as $\Delta\text{GMT}_{\text{GHG}}$). We can also calculate ΔAMOC from the feedback loop in this GHG-driven experiment where there is no direct AMOC driving:

$$\begin{aligned}\Delta\text{AMOC} &= \alpha * \Delta\text{GMT}_{\text{GHG}} + \alpha * \alpha\beta * \Delta\text{GMT}_{\text{GHG}} + ... \\ &= \alpha * \Delta\text{GMT}_{\text{GHG}}/(1 - \alpha\beta)\end{aligned}$$

Within the greenhouse gas forced SSP scenarios, therefore:

$$\Delta\text{AMOC} = \alpha * \Delta\text{GMT}_{\text{Realised}}$$

We can therefore perform a linear regression of AMOC on global annual mean temperature as calculated from a given climate model and use this to calculate an estimate for the impact of GMT on AMOC (α) (Panel A, Supplementary Figure 1).

5.3.2 Impact of AMOC on GMT

For the influence of the Atlantic Meridional Overturning Circulation on the Global Mean Temperature, we can perform a similar analysis in a scenario where we intervene on the AMOC through freshwater forcing. In this case, we have a direct change of the AMOC, which is then adjusted through feedback. This gives the equation:

$$\begin{aligned}\Delta\text{GMT}_{\text{Realised}} &= \beta * \Delta\text{AMOC}_{\text{Driv}} + \beta * \alpha\beta * \Delta\text{AMOC}_{\text{Driv}} + ... \\ &= \beta * \Delta\text{AMOC}_{\text{Driv}}/(1 - \alpha\beta)\end{aligned}$$

Using an equivalent adjustment to the previous section for the feedback impact on AMOC: $\Delta\text{AMOC} = \Delta\text{AMOC}_{\text{Driv}}/(1 - \alpha\beta)$. Therefore:

$$\Delta\text{GMT}_{\text{Realised}} = \beta * \Delta\text{AMOC}$$

We can therefore regress the change in the observed global mean temperature on the AMOC for ClimTip and NAHosMIP freshwater hosing scenarios and this will give us estimates of the impact of AMOC change on GMT (β) (Panel B, Supplementary Figure 1).

5.3.3 Impact of AMOC on Regional Mean Temperature

To calculate the impact of changes in the Atlantic Meridional Overturning Circulation (AMOC) on regional mean temperature (RMT), the RMT was regressed on the change in AMOC for the NAHosMIP and ClimTip runs (Supplementary Figure 2). This was done using annual mean data.

For this analysis, the volume flux change of AMOC was used to estimate the impact of AMOC on regional mean temperature. It was assumed that the initial value of the AMOC did not affect the regional mean temperature behaviour and that the fractional change or other non-linear relationships were not important. This rested on the assumption that the change in volume flux would be most informative for the change in the meridional heat transport, rather than using a fractional change in the AMOC which might correspond to very different changes in heat flux for different models and mean states. While some non-linear impacts could be expected (particularly in regional responses due to changes in specific convection sites) [24], this analysis only includes eleven hosing experiments (of which eight are included in the main analysis). These experiments have very different representations of the convection regions [6] and it is therefore difficult to extract more complex relationships between AMOC and regional mean temperatures across the ensemble. Linear relationships are therefore assumed.

Area-weighted regional mean temperatures are regressed on the change in Atlantic Meridional Overturning Circulation strength to calculate δ.

5.3.4 Impact of Global Temperature on Regional Temperature

The final element in the framework is the relationship between global and regional mean temperatures with the AMOC held constant (Supplementary Figure 3). This is calculated using estimates of both temperatures adjusted for the influence of a changing AMOC. ($\Delta\text{GMT}_{\text{GHG}}$) is a proxy for the influence of greenhouse gas/ radiative forcing on global surface temperature and is calculated by adjusting the realised GMT to take account of feedbacks with the AMOC (as described in Section 5.3.1):

$$\Delta\text{GMT}_{\text{Realised}} = \Delta\text{GMT}_{\text{GHG}}/(1 - \alpha\beta)$$

The adjusted regional mean temperature is calculated by subtracting an estimate of the regional mean temperature change due to AMOC from the realised regional mean

temperature:

$$\begin{aligned}\Delta\text{RMT}_{\text{GHG}} &= \Delta\text{RMT}_{\text{Realised}} - \Delta\text{RMT}_{\text{AMOC}} \\ &= \Delta\text{RMT}_{\text{Realised}} - \delta * \Delta\text{AMOC}\end{aligned}$$

The values for GMT, RMT, and AMOC are all taken from a given CMIP6 SSP245 model run. The value for α is taken from the same run and the values for β and δ are taken from a hosing run of the same model. By calculating the adjusted values for $\Delta\text{RMT}_{\text{GHG}}$ and $\Delta\text{GMT}_{\text{GHG}}$ we then regress these together to calculate γ.

$$\Delta\text{RMT}_{\text{GHG}} = \gamma * \Delta\text{GMT}_{\text{GHG}}$$

5.3.5 Linearity

In this study, a linear relationship is assumed between changes in the AMOC, GMT, and RMT. Although some non-linear responses may be expected due to the non-linear nature of the climate system, in all the data analysed from the models in this study, linear relationships appear to capture the vast majority of the behaviour, with no significant evidence of quadratic or further non-linear behaviour. This can be seen in the plots of GMT and RMT vs AMOC and the plots of AMOC and RMT vs GMT in Figure 2 and the equivalent figures for the other models (Supplementary Figures 4-9). These figures provide insufficient evidence to justify a different functional form and so this study retains the linear assumption, future research may support a relaxation of this assumption.

5.3.6 State Dependence of Relationships

Some studies have suggested dependence of some relationships in this framework on the state of the GMT or AMOC [24]. However, these have often focused on single model studies, and the lack of consistent non-linearity across the ensemble for all the relationships in the framework (as described in the previous subsection), suggest that the relationships are not dependent on the state of the AMOC or GMT as otherwise the changing state would be expected to introduce non-linearities.

For the impact of AMOC on RMT and GMT, the ClimTip and NAHosMIP hosing runs can be compared as they use the same freshwater hosing but the NAHosMIP runs do this under pre-industrial GMT while the ClimTip runs are at 2°C warming. The responses of RMT and GMT are not consistently stronger or weaker at either temperature level, which provides no evidence for non-linearities in the relationship due to changing GMT. For GMT, the ClimTip responses are well within the range of the larger NAHosMIP ensemble (Supplementary Figure 1). For RMT, the ClimTip responses are not consistently weaker or stronger than the NAHosMIP experiments. Looking at specific models, in HadGEM3-GC31-MM the RMT and GMT response to AMOC is stronger under pre-industrial conditions than at 2°C warming, while MPI-ESM1-2-HR shows a weaker response. Therefore, there is no evidence in this ensemble to support a state-dependent temperature response to AMOC, and a linear relationship will be assumed.

5.4 Projections

Once the framework parameters are calculated, projections of the RMT impacts of given scenarios can be produced. This is done by choosing trajectories for the future change in GMT and AMOC (which can be taken from climate models, expert elicitation, or any other source) and inputting them into the following equation:

$$\Delta\mathrm{RMT}_{\mathrm{Realised}} = \gamma * \Delta\mathrm{GMT}_{\mathrm{GHG}} + \delta * \Delta\mathrm{AMOC} = \gamma(1 - \alpha\beta) * \Delta\mathrm{GMT}_{\mathrm{Realised}} + \delta * \Delta\mathrm{AMOC}$$

Here we use CMIP6 SSP245 $\Delta\mathrm{GMT}_{\mathrm{Realised}}$ trajectories combined with a linear reduction in AMOC of 12Sv over the 2015 to 2100 period.

Different methods can be used to source the values α,β,γ,δ and combine them to make these projections. These methods are discussed in the following section.

5.4.1 Offset Method

"Offset Methods" use an estimate of the impact of AMOC change and offset this from an existing climate change scenario. This is often done using a single model estimate, without accounting for the AMOC change already present in the climate change scenario. We imitate this approach for comparison with results from the framework developed in this study using multi-model mean value of δ and projecting regional mean temperature as:

$$\Delta\mathrm{RMT}_{\mathrm{Projected}} = \Delta\mathrm{RMT}_{\mathrm{Realised}} + \delta * \Delta\mathrm{AMOC}$$

This approach double counts some of the change in AMOC (as it doesn't consider AMOC change that has already occurred in the climate change scenario) and neglects structural model uncertainty in the AMOC-RMT relationship.

5.4.2 Individual Projections

The basic setup for this framework uses the equation given in Section 5.4 for the projections and takes the estimates for α,β,γ,δ from a single model. These parameters are then combined with a single global mean temperature pathway from an SSP245 scenario of the same model, and the chosen AMOC pathway and this is used to project the regional mean temperature. In cases where there is more than one ensemble member for a given model and warming scenario, the α,β,γ,δ values calculated for each ensemble member are combined with GMT trajectories from all ensemble members, to explore a greater range of uncertainty. When these models are combined to produce an overall distribution (e.g. Fig 3 Individual Projections) the models are weighted equally to avoid models with additional ensemble members dominating the distribution.

5.4.3 Distributions

Finally, statistical distributions are fitted to the parameters produced by the models and ensemble members. For each distribution, values for α,β, and γ are drawn from the distribution. As β and δ have an exceptionally strong correlation of 99% (Supplementary Figure 14) this is reflected in the framework by selecting a value for δ from

the value of β given by the distribution, using this strong correlation relationship. These parameters are then combined with GMT trajectories from the models and the hypothetical AMOC pathway, and used to project regional mean temperatures with the equation given in Section 5.4. The distributions utilised in this analysis are a uniform distribution covering the full range of parameters calculated from the ensemble, a normal distribution fit to match the mean and standard deviation of the ensemble, and a gamma distribution also fit to the calculated parameter but with the location parameter set to zero to force a single-sign output (where this may be desirable for physical reasons).

5.4.4 Removing Extreme Models

To explore the impact of model choice on uncertainty, we repeated the analysis but with the two most extreme models removed (the models with the highest values for δ). These models were CESM2 and IPSL-CM6A-LR (as shown in Table 1). The remaining ensemble of models was then analysed in the same way as described in each of the subsections above.

Supplementary information. This article is accompanied by Supplementary Information containing a list of the models, experiments and variants used to produce this analysis. It also contains figures demonstrating the regression analysis used to produce the parameters in the framework for models other than CanESM5 (as in Figure 2). It has figures demonstrating the correlations between parameters across the model ensemble. It shows the regional temperature impacts of a 12 Sv AMOC decline as in Figure 3 but for other IPCC AR6 Regions.

Declarations

Funding

This is ClimTip contribution #182; the ClimTip project has received funding from the European Union's Horizon Europe research and innovation programme under grant agreement No. 101137601: Funded by the European Union. Views and opinions expressed are however those of the author(s) only and do not necessarily reflect those of the European Union or the European Climate, Infrastructure and Environment Executive Agency (CINEA). Neither the European Union nor the granting authority can be held responsible for them.

The authors acknowledge the Forecasting Tipping Points programme of the Advanced Research + Invention Agency (ARIA) for the RobustAssess (SCOP-PR01-P029) project.

Conflict of Interest

The authors declare no conflict of interest

Data Availability

CMIP6 data analysed in this are available from the ESGF portal: https://esgf-node.ipsl.upmc.fr/projects/cmip6-ipsl/ NAHosMIP data is available from Zenodo[40]. ClimTip data is available from Zenodo [41] .

Code Availability

Code used for data processing, analysis, and production of figures is available at: https://github.com/JonathanRosser/Uncertainties-in-the-Regional-Consequences-of-AMOC-Reductions

Author Contribution

J.P.R. and D.S. conceived and designed the study. J.P.R. processed the data, wrote the code, performed the analysis and drafted the figures. J.P.R. and D.S. drafted the original manuscript.

References

[1] Dietz, S., Rising, J., Stoerk, T. & Wagner, G. Economic impacts of tipping points in the climate system. *Proceedings of the National Academy of Sciences* **118**, e2103081118 (2021).

[2] Lenton, T. M. *et al.* Global tipping points report 2025 (2025).

[3] van Westen, R. M. & Baatsen, M. L. European temperature extremes under different amoc scenarios in the community earth system model. *Geophysical Research Letters* **52**, e2025GL114611 (2025).

[4] Schaumann, F. & Alastrué de Asenjo, E. Weakening amoc reduces ocean carbon uptake and increases the social cost of carbon. *Proceedings of the National Academy of Sciences* **122**, e2419543122 (2025).

[5] Baker, J. *et al.* Continued atlantic overturning circulation even under climate extremes. *Nature* **638**, 987–994 (2025).

[6] Drijfhout, S., Angevaare, J. R., Mecking, J., van Westen, R. M. & Rahmstorf, S. Shutdown of northern atlantic overturning after 2100 following deep mixing collapse in cmip6 projections. *Environmental Research Letters* **20**, 094062 (2025).

[7] Rahmstorf, S. Is the atlantic overturning circulation approaching a tipping point? *Oceanography* **37**, 16–29 (2024).

[8] Jackson, L. C. *et al.* Challenges simulating the amoc in climate models. *Philosophical Transactions of the Royal Society A* **381**, 20220187 (2023).

[9] Liu, W., Xie, S.-P., Liu, Z. & Zhu, J. Overlooked possibility of a collapsed atlantic meridional overturning circulation in warming climate. *Science Advances* **3**, e1601666 (2017).

[10] Bonan, D. B. *et al.* Observational constraints imply limited future atlantic meridional overturning circulation weakening. *Nature Geoscience* **18**, 479–487 (2025).

[11] Portmann, V., Swingedouw, D., Khattab, O. & Chavent, M. Observational constraints project a˜ 50% amoc weakening by the end of this century. *Science Advances* **12**, eadx4298 (2026).

[12] O'Neill, B. C. *et al.* The scenario model intercomparison project (scenariomip) for cmip6. *Geoscientific Model Development* **9**, 3461–3482 (2016).

[13] Jackson, L. *et al.* Global and european climate impacts of a slowdown of the amoc in a high resolution gcm. *Climate dynamics* **45**, 3299–3316 (2015).

[14] Jackson, L. C. *et al.* Understanding amoc stability: The north atlantic hosing model intercomparison project. *Geoscientific Model Development* **16**, 1975–1995 (2023).

[15] Nowicki, S. M. *et al.* Ice sheet model intercomparison project (ismip6) contribution to cmip6. *Geoscientific model development* **9**, 4521–4545 (2016).

[16] Schmidt, G. A. *et al.* Datasets and protocols for including anomalous freshwater from melting ice sheets in climate simulations. *Geoscientific Model Development* **18**, 8333–8361 (2025).

[17] Mecking, J., Drijfhout, S., Jackson, L. & Andrews, M. The effect of model bias on atlantic freshwater transport and implications for amoc bi-stability. *Tellus A: Dynamic Meteorology and Oceanography* **69**, 1299910 (2017).

[18] Van Westen, R. M. & Dijkstra, H. A. Persistent climate model biases in the atlantic ocean's freshwater transport. *Ocean Science* **20**, 549–567 (2024).

[19] Winkelmann, R. *et al.* The tipping points modelling intercomparison project (tipmip): Assessing tipping point risks in the earth system. *Earth System Dynamics Discussions* (2025).

[20] Jones, C. *et al.* The tipmip earth system model experiment protocol: phase 1. *Geoscientific Model Development Discussions (GMDD)* (2025).

[21] Swingedouw, D. *et al.* Tipmip-ocean experimental protocol phase 1: Tipping dynamics of the amoc. *EGUsphere* **2026**, 1–36 (2026).

[22] Eyring, V. *et al.* Overview of the coupled model intercomparison project phase 6 (cmip6) experimental design and organization. *Geoscientific Model Development*

9, 1937–1958 (2016).

[23] Dijkstra, H. A. *et al.* Multi-stability of the present-day atlantic meridional overturning circulation. *Wiley Interdisciplinary Reviews: Climate Change* **17**, e70049 (2026).

[24] Bellomo, K. & Mehling, O. Impacts and state-dependence of amoc weakening in a warming climate. *Geophysical research letters* **51**, e2023GL107624 (2024).

[25] Drijfhout, S. Competition between global warming and an abrupt collapse of the amoc in earth's energy imbalance. *Scientific reports* **5**, 14877 (2015).

[26] Caesar, L., Rahmstorf, S. & Feulner, G. On the relationship between atlantic meridional overturning circulation slowdown and global surface warming. *Environmental Research Letters* **15**, 024003 (2020).

[27] van Westen, R. M., Vanderborght, E., Kliphuis, M. & Dijkstra, H. A. Physics-based indicators for the onset of an amoc collapse under climate change. *Journal of Geophysical Research: Oceans* **130**, e2025JC022651 (2025).

[28] Weijer, W., Cheng, W., Garuba, O. A., Hu, A. & Nadiga, B. T. Cmip6 models predict significant 21st century decline of the atlantic meridional overturning circulation. *Geophysical Research Letters* **47**, e2019GL086075 (2020).

[29] Ditlevsen, P. & Ditlevsen, S. Warning of a forthcoming collapse of the atlantic meridional overturning circulation. *Nature communications* **14**, 4254 (2023).

[30] Iturbide, M. *et al.* An update of ipcc climate reference regions for subcontinental analysis of climate model data: definition and aggregated datasets. *Earth System Science Data* **12**, 2959–2970 (2020).

[31] Katzav, J. *et al.* On the appropriate and inappropriate uses of probability distributions in climate projections and some alternatives. *Climatic Change* **169**, 15 (2021).

[32] Frigg, R., Smith, L. A. & Stainforth, D. A. The myopia of imperfect climate models: the case of ukcp09. *Philosophy of science* **80**, 886–897 (2013).

[33] Frigg, R., Smith, L. A. & Stainforth, D. A. An assessment of the foundational assumptions in high-resolution climate projections: the case of ukcp09. *Synthese* **192**, 3979–4008 (2015).

[34] Stainforth, D. A., Downing, T. E., Washington, R., Lopez, A. & New, M. Issues in the interpretation of climate model ensembles to inform decisions. *Philosophical Transactions: Mathematical, Physical and Engineering Sciences* 2163–2177 (2007).

[35] Link, P. M. & Tol, R. S. Estimation of the economic impact of temperature changes induced by a shutdown of the thermohaline circulation: an application of fund. *Climatic Change* **104**, 287–304 (2011).

[36] Tebaldi, C. & Knutti, R. The use of the multi-model ensemble in probabilistic climate projections. *Philosophical Transactions: Mathematical, Physical and Engineering Sciences* 2053–2075 (2007).

[37] Stainforth, D. A. *et al.* Uncertainty in predictions of the climate response to rising levels of greenhouse gases. *Nature* **433**, 403–406 (2005).

[38] Parker, W. S. Ensemble modeling, uncertainty and robust predictions. *Wiley interdisciplinary reviews: Climate change* **4**, 213–223 (2013).

[39] Lawrence, B. N. *et al. Storing and manipulating environmental big data with jasmin*, 68–75 (IEEE, 2013).

[40] Jackson, L. *et al.* Nahosmip data (2023). URL https://doi.org/10.5281/zenodo.7643437.

[41] Bathiany, S. Climtip esm simulations d7.1 & d8.1 - monthly data, version 3.0 (2026). URL https://doi.org/10.5281/zenodo.20324954.

Supplementary Files

This is a list of supplementary files associated with this preprint. Click to download.

- AMOCPaperActiveVersionSI.pdf